

# Comprehensive Chemical Characterization of Complexes Involving Lead-Amino Acid Interactions

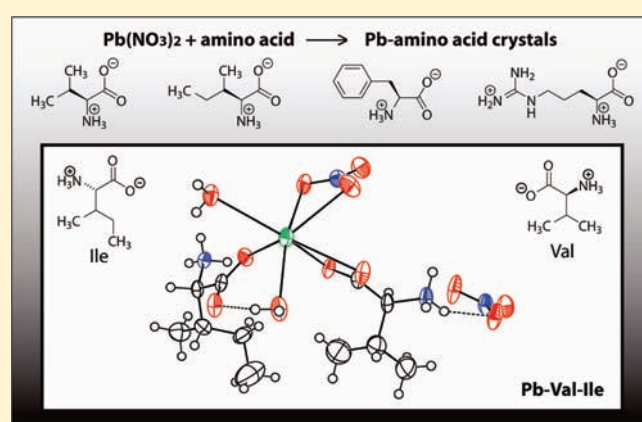
Cheryl D. L. Saunders,<sup>†</sup> Lauren E. Longobardi,<sup>†</sup> Neil Burford,<sup>\*,†</sup> Michael D. Lumsden,<sup>‡</sup> Ulrike Werner-Zwanziger,<sup>‡</sup> Banghao Chen,<sup>†</sup> and Robert McDonald<sup>§</sup>

<sup>†</sup>Department of Chemistry and <sup>‡</sup>Nuclear Magnetic Resonance Research Resource, Dalhousie University, Halifax, Nova Scotia B3H 4J3, Canada

<sup>§</sup>X-ray Crystallography Laboratory, Department of Chemistry, University of Alberta, Edmonton, Alberta T6G 2G2, Canada

**S** Supporting Information

**ABSTRACT:** Complexes of lead with L-phenylalanine, L-isoleucine, L-valine, or L-arginine have been isolated from reaction mixtures containing lead nitrate and the respective amino acid in acidic aqueous solution. The compounds have been comprehensively characterized using X-ray crystallography, solid state NMR spectroscopy and solution state NMR spectroscopy, IR and Raman spectroscopies, and electrospray ionization mass-spectrometry. The solid state structures of lead-phenylalanine, lead-valine, and lead-valine-isoleucine complexes show a lead center coordinated by two amino acid ligands, while the lead-arginine complex is a cluster involving two lead centers and three arginine molecules. The structural, spectroscopic, and spectrometric characterization of the complexes provides a basis to establish a fundamental understanding of heavy metal-amino acid interactions.

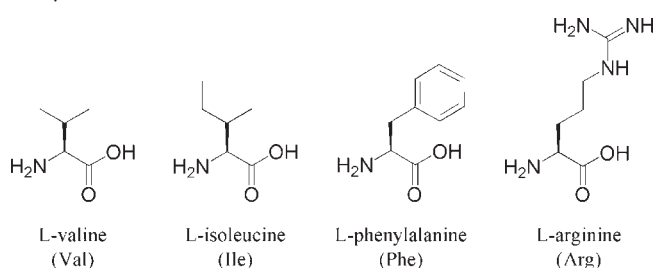


## INTRODUCTION

The anthropic use of lead as a functional and inert metal for over a millennium revealed a substantial negative bioactivity that was first described by Hippocrates in 370 BC.<sup>1</sup> Although ions of heavy metals are expected to interact with many bioligands, complexes formed between heavy metals and amino acids, peptides or proteins likely have the most dramatic physiological consequences. Limited characterization data is available for complexes of lead with amino acid ligands, precluding meaningful comparisons and the development of a self-consistent model for such interactions. Crystallographic data has been reported for complexes of lead with aspartic acid,<sup>2</sup> phenylalanine,<sup>3</sup> isoleucine,<sup>4</sup> and proline,<sup>5</sup> as well as for the nonbiological amino acids D-penicillamine<sup>6</sup> and 3,5-dinitrotyrosine.<sup>7</sup> The data is often specific to an isolated crystal and may or may not be relevant to the solution behavior of the compound. The identity and structure of some complexes have been proposed on the basis of solution state NMR data<sup>8</sup> and IR data.<sup>9,10</sup>

We now describe the isolation of nitrate salts of the first complexes of lead with L-valine (Val),<sup>11</sup> L-phenylalanine (Phe), or L-arginine (Arg), as well as a complex involving both L-valine and L-isoleucine. In addition, we present comparative data for the complex of L-isoleucine (Ile).<sup>4</sup> These compounds have been comprehensively characterized using X-ray crystallography, solid state NMR spectroscopy and solution state NMR spectroscopy, IR and Raman spectroscopies, and electrospray ionization mass-spectrometry.

The results provide a basis to establish a fundamental understanding of heavy metal-amino acid interactions.



## EXPERIMENTAL SECTION

**Caution!** Compounds of lead are highly toxic. Care must be taken when handling samples, and appropriate disposal procedures are necessary.

**General Procedures.** L-arginine, L-isoleucine, L-phenylalanine, L-valine, sodium 2,2-dimethyl-2-silapentane-5-sulfonate (DSS; also known as sodium 3-trimethylsilylanyl-propane-1-sulfonate), deuterium chloride (99 atom % D, 37 wt % solution in D<sub>2</sub>O), deuterated nitric acid (99+ atom % D, 65 wt % solution in D<sub>2</sub>O), sodium deuteroxide 99+ atom % D, 40 wt % solution in D<sub>2</sub>O), sodium nitrate, mercury(I) nitrate

**Received:** September 17, 2010

**Published:** March 09, 2011

dihydrate, mercury(II) nitrate hydrate were used as received from Aldrich. Potassium chloride was used as received from ACP Chemicals, Inc. *N*-Methyl-L-alanine was used as received from Fluka. Lead nitrate was used as received from BDH. Nitric acid was used as received from Caledon. Deuterium oxide was used as received from Cambridge Isotopes Laboratories (99.9 atom % D) and Aldrich (99.9 atom % D). Deionized water was used in all reactions, and crystallization procedures and all procedures were carried out in air, unless otherwise indicated.

Samples for IR spectroscopy were prepared as Nujol mulls between CsI disks. Samples for Raman spectroscopy were ground into fine powders and packed into glass capillary tubes. Raman data were collected on a Bruker RFS 100 FT-Raman Spectrometer (Nd:YAG laser, emission wavelength 1.06  $\mu\text{m}$ , output power 80 mW). IR data were collected on a Bruker Vector 22 spectrometer (He:Ne laser, emission wavelength 633 nm, output power 1 mW) or a PerkinElmer precisely Spectrum 100 FT-IR spectrometer (source type: MIR; detector type: LiTaO<sub>3</sub>).

Samples for solid state <sup>13</sup>C and <sup>207</sup>Pb NMR spectroscopy were ground into a fine powder and packed in a 4 mm rotor. All experiments were carried out on a Bruker Avance NMR spectrometer with a 9.4 T magnet (400 MHz proton Larmor frequency, 100.6 MHz <sup>13</sup>C Larmor frequency, 83.6 MHz <sup>207</sup>Pb Larmor frequency) or on a Bruker Avance NMR spectrometer with a 16.4 T magnet (700 MHz proton Larmor frequency, 176.1 MHz <sup>13</sup>C Larmor frequency).

For carbon-13 solid state NMR analyses, the samples were spun at different spinning speeds between 7.0 kHz and 10.0 kHz to distinguish center bands from spinning sidebands. Relaxation times for the protons were determined by inversion recovery sequences. From these experiments recycle delays between 5 s and 10.00 s were employed for the <sup>13</sup>C cross-polarization (CP)/magic angle spinning (MAS) experiments. The other parameters for the <sup>13</sup>C CP/MAS experiments with TPPM proton decoupling were optimized on glycine, whose carbonyl resonance also served as external, secondary chemical shift standard at 176.06 ppm. For the <sup>13</sup>C CP/MAS NMR spectra between 16 and 120 scans were accumulated, using 2.6 ms CP contact times and ramped proton powers.

The <sup>207</sup>Pb solid state NMR spectra were acquired with Single Pulse Excitation (SPE) (with pulse length of 90 degrees on resonance). The samples were spun at various spinning speeds between 10 and 13 kHz to determine center bands and to identify spinning sidebands. Relaxation times were not determined. Repetition times between 1 and 12 s were used. Between 2000 and 9000 transients were accumulated. The spectra are baseline corrected. The large chemical shift anisotropies made it necessary to vary the rf-excitation frequency to cover the full range of spinning sidebands and to faithfully characterize the isotropic chemical shifts. Chemical shift referencing was done with solid Pb(NO<sub>3</sub>)<sub>2</sub>. Its temperature dependence has been well characterized.<sup>12</sup> Because of spinning induced sample heating, which is not known to sufficient precision, a static powder sample was used with the temperature read from a temperature sensor. Fitting the obtained line shape with the program *xedplot*<sup>13</sup> and the value of the isotropic shift given in the paper above, the chemical shift was referenced. This value was compared with the Pb(NO<sub>3</sub>)<sub>2</sub> spinning at 5 and 10 kHz including spinning induced temperatures following described procedures.<sup>14</sup> The three values obtained were consistent. An uncertainty in the shift of 2 ppm was added to the results. No change in reference frequency was observed over the experimental time.

For [Pb(OH<sub>2</sub>)<sub>2</sub>(Val)(Ile)(NO<sub>3</sub>)][NO<sub>3</sub>], spectra were acquired with both Single Pulse Excitation (SPE) (with pulse length of 90 degree on resonance) and Hahn echoes. A 20  $\mu\text{s}$  Hahn echo pulse delay was chosen and was sufficient for whole echo acquisition. Consequently, the spectra can be viewed in magnitude mode. For direct comparison with the other spectra, we show the spectrum acquired with single pulse excitation.

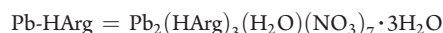
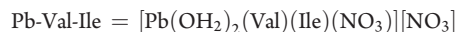
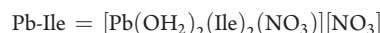
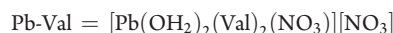
pH and pD measurements for reaction mixtures were performed using a ROSS Sure-Flow combination pH electrode with a

ThermoOrion model 230 pH meter. pD measurements for the smaller dissolved crystal samples were performed using ISFET Sensor Probe T2-387 PH 47-SS, I.Q. Scientific Instruments. For the pD measurements, the ROSS Sure-Flow electrode was soaked overnight in a 0.67 M KCl in deuterium oxide solution, while the ISFET Sensor Probe was initially soaked for 30 min in deuterium oxide (to hydrate the probe) and then soaked for an additional 20 min in the 0.67 M KCl in deuterium oxide solution. Details regarding probe calibration are presented in the Supporting Information.

NMR samples of lead-amino acid reaction mixtures were prepared under nitrogen gas by stirring the mixture in deuterium oxide at room temperature until clear (ca. 5 to 10 min) in 5.00 mL volumes and 0.125 M concentrations of amino acid or lead. The pD of the solution was measured. DSS was added to a 1.00 mL aliquot of each sample to a concentration of  $1.0 \times 10^{-2}$  M DSS. NMR samples of crystalline solids dissolved in deuterium oxide were prepared at 0.125 M in 1.00 mL by stirring at room temperature until the solid completely dissolved. The pD of the solution was measured. DSS was added to each solution to give a concentration of  $1.0 \times 10^{-2}$  M DSS.<sup>15</sup>

Electrospray ionization mass spectra (ESI-MS) of lead-amino acid reaction mixtures were obtained on aliquots of the filtrates that were diluted in distilled water and also in 50/50 (v/v) methanol/distilled water (final concentration  $1.25 \times 10^{-2}$  M). Positive and negative ion ESI-MS spectra were obtained using a Finnigan LCQ DUO ion trap mass spectrometer. Two separate flow solvents were used, distilled water and 50/50 (v/v) methanol/distilled water. Instrument parameters were set at: 1.2 mL/h for the flow solvent rate, 4.00 kV for the spray voltage, 200 °C for the capillary temperature, and the in-source fragmentation option was not activated. The relative abundance of each peak for each sample type was reproducible within the ranges H (75% to 100%), M (35% to 75%), L (5% to 35%), or V (<5%). To verify the ion identity for each spectral peak, the experimentally observed isotope peak patterns were compared to calculated isotope patterns using Isotope Pattern Calculator v 4.0.<sup>16</sup> In addition, tandem mass spectrometric analysis of the more abundant ions in each solution was also performed. All spectra were analyzed and processed using: Qual Browser,<sup>17</sup> Microsoft Excel 2002,<sup>18</sup> and Sigma Plot.<sup>19</sup>

The acquisition of meaningful elemental analysis data was precluded by the presence of lattice water in all isolated samples. Chemical formulas given for the complexes are based on the asymmetric unit observed in the crystal structures, where ligands directly bonded to the lead center(s) are written within the first square brackets, the nonlead bonded nitrate ion is contained in the second set of square brackets, and any additional water molecules are written as solvate. Abbreviations of the formulas listed below are used for clarity in some tables and figures.



### Isolation Procedures and Characterization Data

**Pb-Val.** A stirred solution (10 min) of L-valine (5.00 mmol, 0.586 g) in water (10 mL, pH 6.38) was added to a solution of Pb(NO<sub>3</sub>)<sub>2</sub> (5.00 mmol, 1.656 g) in water (30 mL, stirred 10 min, pH 3.73) resulting in a clear, colorless solution with a pH of 4.30. The mixture was heated at

Table 1. Crystallographic Data for Lead-Amino Acid Complexes<sup>a,b</sup>

	Pb-Val	Pb-Val-Ile	Pb-Phe·2H <sub>2</sub> O	Pb-HArg
empirical formula	C <sub>10</sub> H <sub>26</sub> N <sub>4</sub> O <sub>12</sub> Pb	C <sub>11</sub> H <sub>28</sub> N <sub>4</sub> O <sub>12</sub> Pb	C <sub>18</sub> H <sub>26</sub> N <sub>4</sub> O <sub>12</sub> Pb	C <sub>18</sub> H <sub>53</sub> N <sub>19</sub> O <sub>31</sub> Pb <sub>2</sub>
FW	601.54	615.56	697.62	1446.17
crystal dimensions	0.52 × 0.51 × 0.20	0.44 × 0.35 × 0.16	0.63 × 0.16 × 0.12	0.63 × 0.23 × 0.11
crystal system	orthorhombic	orthorhombic	orthorhombic	monoclinic
space group	P2 <sub>1</sub> 2 <sub>1</sub> 2 <sub>1</sub> (No. 19)	P2 <sub>1</sub> 2 <sub>1</sub> 2 <sub>1</sub> (No. 19)	P2 <sub>1</sub> 2 <sub>1</sub> 2 <sub>1</sub> (No. 19)	P2 <sub>1</sub> (No. 4)
<i>a</i> (Å)	5.4125 (6)	5.4526 (4)	5.3525 (4)	7.4258 (7)
<i>b</i> (Å)	13.6907 (14)	13.5911 (11)	13.4886 (10)	28.522 (3)
<i>c</i> (Å)	26.708 (3)	28.742 (2)	33.906 (3)	10.8529 (10)
<i>V</i> (Å <sup>3</sup> )	1979.1 (4)	2130.0 (3)	2447.9 (3)	2259.4 (4)
<i>Z</i>	4	4	4	2
$\rho_{\text{calcd}}$ (g cm <sup>-3</sup> )	2.019	1.920	1.893	2.126
$\mu$ (mm <sup>-1</sup> )	8.590	7.984	6.960	7.561
2 $\theta$ limit(deg)	54.96	57.20	54.94	55.02
total number of data collected	16494	18904	51445	19964
	-7 ≤ <i>h</i> ≤ 7	-7 ≤ <i>h</i> ≤ 7	-6 ≤ <i>h</i> ≤ 6	-9 ≤ <i>h</i> ≤ 9
	-17 ≤ <i>k</i> ≤ 17	-17 ≤ <i>k</i> ≤ 17	-17 ≤ <i>k</i> ≤ 17	-37 ≤ <i>k</i> ≤ 36
	-34 ≤ <i>l</i> ≤ 34	-37 ≤ <i>l</i> ≤ 37	-43 ≤ <i>l</i> ≤ 44	-14 ≤ <i>l</i> ≤ 14
number of independent reflections	4510	5141	5571	10295
<i>R</i> <sub>int</sub>	0.0246	0.0302	0.0243	0.0210
number of observed reflections	4061	4941	5463	9931
range of transmission factors	0.2784–0.0945	0.3615–0.1270	0.4889–0.0967	0.4901–0.0872
number of data/restraints/params	4510/0/244	5141/0/253	5571/0/316	10295/0/634
Flack absolute structure parameter	0.001 (5)	0.043(7)	0.010 (7)	0.002 (3)
<i>R</i> <sub>1</sub> [ <i>F</i> <sub>o</sub> <sup>2</sup> ≥ 2σ( <i>F</i> <sub>o</sub> <sup>2</sup> )]	0.0181	0.0253	0.0254	0.0218
w <i>R</i> <sub>2</sub> [all data]	0.0406	0.0589	0.0588	0.0470
GOF [all data]	1.047	1.150	1.140	0.968

<sup>a</sup> Distances involving the hydrogen atoms of the water molecules were given fixed values. <sup>b</sup> Distances involving two hydrogen atoms of the water molecules were given fixed values: *d*(O2–H2OA) = *d*(O2–H2OB) = *d*(O3–H3OA) = *d*(O3–H3OB) = 0.86 Å; *d*(H2OA···H2OB) = *d*(H3OA···H3OB) = 1.40 Å. Idealized hydrogen-bonded geometries for these water molecules were achieved by constraining the hydrogen atoms to lie in the same plane as the oxygen atoms to which they are bonded and hydrogen-bonded, i.e., by constraining the five-atom units ([a] O32···H2OA–O2–H2OB···O3[at 1+*x*, *y*, *z*]; [b] O21···H3OA–O3–H3OB···O31[at 1–*x*, –1/2+*y*, 1/2–*z*]) to define a polyhedron with a volume of no more than 0.05 Å<sup>3</sup>.

95–100 °C for 60 min and slowly cooled to room temperature in the filtration flask. Colorless needle-like crystals of [Pb(OH<sub>2</sub>)<sub>2</sub>(Val)<sub>2</sub>(NO<sub>3</sub>)][NO<sub>3</sub>] formed over 4 days at room temperature; yield: 0.684 g; 45.5%; mp 88–92 °C. **Solid** <sup>13</sup>C CP-MAS NMR  $\delta$  (ppm): 175.9, 175.3, 63.8, 62.6, 30.0, 20.4, 19.8; <sup>207</sup>Pb CP-MAS NMR  $\delta$ : –1707 ± 5 ppm; IR (cm<sup>-1</sup>): 3475, 1615, 1514, 1153, 1117, 1057, 1043, 1025, 944, 932, 894, 821, 753, 718, 587, 588, 448, 382, 317; Raman (cm<sup>-1</sup>): 2973, 2898, 1328. **Solution** <sup>13</sup>C NMR  $\delta_{\text{DSS}}$  (ppm, D<sub>2</sub>O; pD = 5.0; 0.125 M Val): 177.4, 63.6, 31.7, 20.6, 19.3; <sup>207</sup>Pb NMR (ppm, D<sub>2</sub>O; pD = 4.9; 0.125 M Pb)  $\delta$ : –2525.

**Pb-Ile.** Previous report of isolation.<sup>4</sup> A stirred mixture (10 min) of L-isoleucine (5.01 mmol, 0.657 g) in water (10 mL pH 6.23) was added to a solution of Pb(NO<sub>3</sub>)<sub>2</sub> (5.00 mmol, 1.657 g) in water (30 mL, stirred 10 min, pH 3.73) resulting in a clear, colorless solution with a pH of 4.30. The solution was heated at 95–100 °C for 60 min. On slow cooling to room temperature in the filtration flask colorless needle-like crystals of [Pb(OH<sub>2</sub>)<sub>2</sub>(Ile)<sub>2</sub>(NO<sub>3</sub>)][NO<sub>3</sub>] formed from the filtrate over 14 days at room temperature; yield: 0.617 g; 39.1%; mp 82–83 °C. **Solid** <sup>13</sup>C CP-MAS NMR  $\delta$  (ppm): 175.9, 62.1, 61.6, 37.2, 35.4, 24.9, 23.6, 16.1, 15.2, 12.6, 10.6; <sup>207</sup>Pb CP-MAS NMR  $\delta$ : –1766 ± 4 ppm; IR (cm<sup>-1</sup>): 3457, 1584, 1505, 1120, 1067, 1044, 1031, 1003, 928, 881, 821, 718, 662, 587, 566, 499, 372, 315; Raman (cm<sup>-1</sup>): 2964, 2938, 2897, 1445. **Solution** <sup>13</sup>C NMR  $\delta_{\text{DSS}}$  (ppm, D<sub>2</sub>O; pD = 4.9; 0.125 M Ile): 177.3, 62.7, 38.5,

27.2, 17.7, 13.8; <sup>207</sup>Pb NMR (ppm, D<sub>2</sub>O; pD = 4.9; 0.125 M Pb)  $\delta$ : –2471.

**Pb-Val-Ile.** A stirred mixture (10 min) of L-valine (5.00 × 10<sup>-3</sup> mmol, 0.586 g) and L-isoleucine (5.02 × 10<sup>-3</sup> mmol, 0.658 g) in water (20 mL, pH 6.21) was added to a solution of Pb(NO<sub>3</sub>)<sub>2</sub> (5.00 × 10<sup>-3</sup> mmol, 1.656 g) in water (20 mL stirred 10 min, pH 3.73) resulting in a clear, colorless solution with a pH of 4.34. The solution was heated at 95–100 °C for 60 min. On slow cooling to room temperature colorless in the filtration flask, needle-like crystals of [Pb(OH<sub>2</sub>)<sub>2</sub>(Val)(Ile)(NO<sub>3</sub>)][NO<sub>3</sub>] formed from the filtrate over 13 days at room temperature; yield: 0.768 g; 25.0%; mp 82–83 °C. **Solid** <sup>13</sup>C CP-MAS NMR  $\delta$  (ppm): 178.8, 76.5, 63.4, 61.7, 36.9, 29.7, 25.2, 23.3, 19.5, 16.4, 15.1, 12.5; <sup>207</sup>Pb CP-MAS NMR  $\delta$  (ppm): ill defined, see Figure 7b; IR (cm<sup>-1</sup>): 3573, 3460, 2448, 2352, 2240, 1924, 1774, 1754, 1614, 1575, 1506, 1260, 1119, 1058, 1044, 1001, 962, 929, 893, 821, 717, 666, 585, 555, 498, 428; Raman (cm<sup>-1</sup>): 2980, 2900, 112. **Solution** <sup>13</sup>C NMR  $\delta_{\text{DSS}}$  (ppm, D<sub>2</sub>O; pD = 4.9; 0.125 M Val and Ile): 177.5, 177.4, 63.8, 62.9, 38.6, 31.8, 27.2, 20.6, 19.4, 17.3, 13.8; <sup>207</sup>Pb NMR (ppm, D<sub>2</sub>O; pD = 4.9; 0.125 M Pb)  $\delta$ : –2471.

**Pb-Phe·2H<sub>2</sub>O.** A stirred (10 min) cloudy white mixture of L-phenylalanine (4.99 mmol, 0.825 g) in water (10 mL pH 5.64) was added to a solution of Pb(NO<sub>3</sub>)<sub>2</sub> (5.00 mmol, 1.657 g) in water (30 mL stirred 10 min, pH 3.73) resulting in a clear, colorless solution with a pH



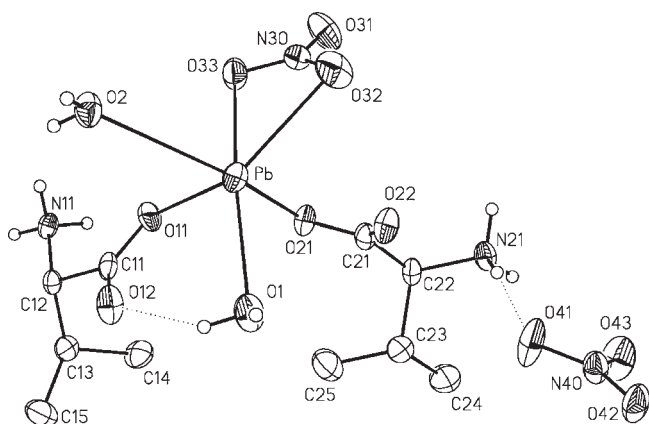


**Figure 1.** Crystallographic view of the asymmetric unit of  $[\text{Pb}(\text{OH}_2)_2(\text{Val})_2(\text{NO}_3)][\text{NO}_3]$ . Non-hydrogen atoms are represented by ellipsoids at the 50% probability level. Hydrogen atoms attached to oxygen or nitrogen atoms are shown with arbitrarily small thermal parameters; all other hydrogen atoms are not shown.

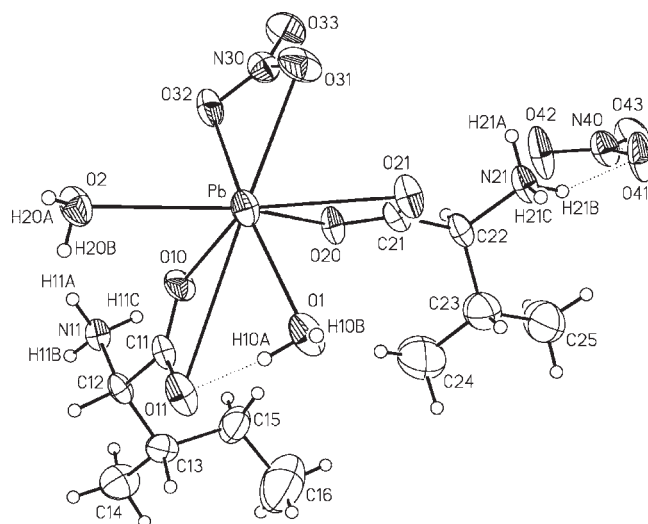


**Figure 2.** Crystallographic view of the asymmetric unit of  $[\text{Pb}(\text{OH}_2)_2(\text{Val})(\text{Ile})(\text{NO}_3)][\text{NO}_3]$ . Non-hydrogen atoms are represented by ellipsoids at the 50% probability level. Hydrogen atoms are shown with arbitrarily small thermal parameters.

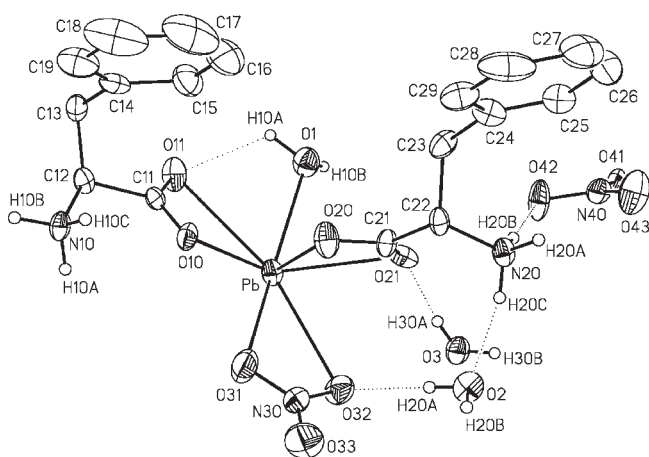


**Figure 3.** Crystallographic views of the asymmetric unit of  $[\text{Pb}(\text{OH}_2)_2(\text{Phe})_2(\text{NO}_3)][\text{NO}_3]$ . Non-hydrogen atoms are represented by ellipsoids at the 50% probability level. Hydrogen atoms attached to oxygen or nitrogen atoms are shown with arbitrarily small thermal parameters; all other hydrogen atoms are not shown.

of 4.02, that was heated at 95–100 °C for 60 min, and the colorless solution became very slightly cloudy. The hot solution was slowly cooled to room temperature in the filtration flask, and colorless needle-like crystals of  $[\text{Pb}(\text{OH}_2)_2(\text{Phe})_2(\text{NO}_3)][\text{NO}_3]$  formed in 4 days at room temperature; yield: 1.112 g; 63.9%; mp 107–110 °C. **Solid**  $^{13}\text{C}$  CP-MAS NMR  $\delta$  (ppm): 235.7, 229.1, 227.6, 226.5, 176.1, 175.2, 136.3, 129.9, 128.1, 127.2, 136.3, 129.8, 128.1, 127.2, 59.7, 58.3, 38.8, 37.7, 30.4, 27.8;  $^{207}\text{Pb}$  CP-MAS NMR  $\delta$  (ppm):  $-1541 \pm 5$ ; IR ( $\text{cm}^{-1}$ ): 3500, 1626, 1566, 1506, 1243, 1135, 1073, 1046, 964, 910, 868, 761 745, 698, 555, 519, 486, 332; Raman ( $\text{cm}^{-1}$ ): 3061, 2932, 1606, 1003, 119. **Solution**  $^{13}\text{C}$  NMR  $\delta_{\text{DSS}}$  (ppm,  $\text{D}_2\text{O}$ ; pD = 5.0; 0.125 M Phe): 177.0, 137.7, 132.0, 131.8, 130.4, 59.1, 38.9;  $^{207}\text{Pb}$  NMR (ppm,  $\text{D}_2\text{O}$ ; pD = 4.7; 0.125 M Pb)  $\delta$ :  $-2536$ .

**Pb-HArg.** A stirred solution (10 min) of L-arginine (5.03 mmol, 0.877 g) in 10 mL of distilled water (pH 11.43) was added to a solution of  $\text{Pb}(\text{NO}_3)_2$  (5.00 mmol, 1.656 g) in 30 mL of distilled water (stirred 10 min) resulting in a cloudy white mixture with a pH of 6.31. This mixture was acidified with concentrated  $\text{HNO}_3$ , with stirring, to pH 3.10 resulting in a clear, colorless solution. This solution was heated at 95–100 °C

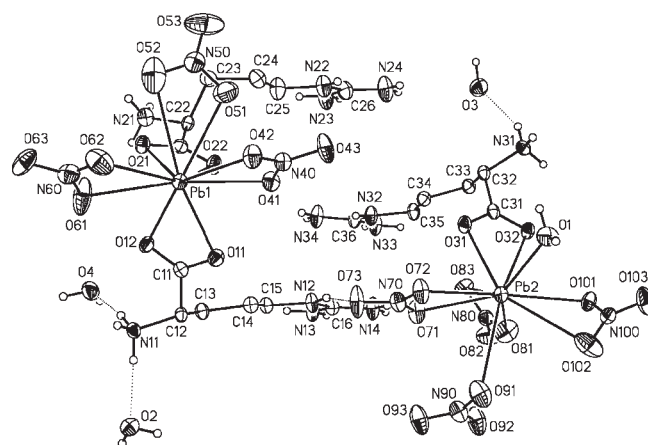


**Figure 4.** Crystallographic view of the asymmetric unit of  $\text{Pb}_2(\text{OH}_2)(\text{HArg})_3(\text{NO}_3)_7 \cdot 3\text{H}_2\text{O}$ . Non-hydrogen atoms are represented by ellipsoids at the 50% probability level. Hydrogen atoms attached to oxygen or nitrogen atoms are shown with arbitrarily small thermal parameters; all other hydrogen atoms are not shown.

for 60 min and was subsequently slowly cooled to room temperature in the filtration flask. Colorless needle-like crystals of  $\text{Pb}_2(\text{Arg}+\text{H})_3(\text{H}_2\text{O})(\text{NO}_3)_7 \cdot 3\text{H}_2\text{O}$  formed from the filtrate in 20 days at room temperature; yield: 0.687 g; 28.3%; mp 92–95 °C. **Solid**  $^{13}\text{C}$  CP-MAS NMR  $\delta$  (ppm): 177.7, 176.6, 157.5, 59.4, 57.6, 56.8, 43.5, 42.7, 40.4, 31.4, 28.4, 24.8, 24.4, 23.3;  $^{207}\text{Pb}$  CP-MAS NMR  $\delta$  (ppm):  $-1285 \pm 5$ ,  $-2511 \pm 5$ ; IR ( $\text{cm}^{-1}$ ): 3189, 1762, 1694, 1587, 1538, 863, 825, 564, 441, 333; Raman ( $\text{cm}^{-1}$ ): 2934, 122. **Solution**  $^{13}\text{C}$  NMR  $\delta_{\text{DSS}}$  (ppm,  $\text{D}_2\text{O}$ ; pD = 4.9; 0.125 M HArg): 177.5, 159.5, 57.5, 43.2, 30.2, 26.6;  $^{207}\text{Pb}$  NMR (ppm,  $\text{D}_2\text{O}$ ; pD = 4.7; 0.125 M Pb)  $\delta$ :  $-2675$ .

When the filtrate evaporated too rapidly a slightly yellow, viscous liquid formed. This liquid was redissolved in 5 mL of distilled water, transferred to a 4 dram vial with a loosely sealed cap and left to slowly evaporate, yielding crystals within 10 days.

**X-ray Crystallography.** Crystals of the metal-amino acid complexes were coated in Paratone-N oil then mounted on a thin glass fiber and cooled to 173(1) K (for Pb-Val-Ile) or 193(2) K (for all other compounds)

Table 2. Selected Pb–O Interatomic Distances (Å) for Lead-Amino Acid Salts Illustrated in Figures 1 to 5<sup>a</sup>

	Pb–O (AA)		Pb–O (NO <sub>3</sub> )		Pb–O (H <sub>2</sub> O)	
[Pb(OH <sub>2</sub> ) <sub>2</sub> (Val) <sub>2</sub> (NO <sub>3</sub> )] [NO <sub>3</sub> ]	O21	2.356(2)			O1	2.512(3)
sphere 1	O11	2.459(2)				
sphere 2	O22	2.892(2)	O33	2.790(3)		
			O32	2.847(3)		
sphere 3	O12	3.266(3)	O31'	2.969(3)	O2	2.915(2)
			O33'	3.174(3)		
[Pb(OH <sub>2</sub> ) <sub>2</sub> (Ile) <sub>2</sub> (NO <sub>3</sub> )] [NO <sub>3</sub> ] <sup>4</sup>	O20	2.379(3)			O1	2.497(3)
sphere 1	O10	2.492(3)				
sphere 2	O21	2.816(2)	O33	2.809(3)		
			O31	2.824(3)		
sphere 3	O11	3.467(3)	O32''	2.934(3)	O2'	2.907(2)
			O33''	3.106(3)		
[Pb(OH <sub>2</sub> ) <sub>2</sub> (Val)(Ile)(NO <sub>3</sub> )] [NO <sub>3</sub> ]	O20	2.379(3)			O1	2.484(4)
sphere 1	O10	2.475(3)				
sphere 2	O21	2.828(3)	O31	2.819(4)	O2	2.886(3)
			O32	2.827(4)		
sphere 3	O11	3.463(4)	O33'	2.925(4)		
			O32'	3.126(3)		
[Pb(OH <sub>2</sub> ) <sub>2</sub> (Phe) <sub>2</sub> (NO <sub>3</sub> )] [NO <sub>3</sub> ]	O20	2.343(3)				
sphere 1	O10	2.442(3)				
sphere 2	O11	2.747(3)	O31	2.857(6)	O1	2.640(4)
					O2	2.871(3)
sphere 3	O21	2.962(3)	O32'	3.016(5)		
			O33	3.033(6)		
			O31'	3.373(3)		
Pb <sub>2</sub> (HArg) <sub>3</sub> (H <sub>2</sub> O)(NO <sub>3</sub> ) <sub>7</sub> ·3H <sub>2</sub> O	O22	2.401(3)				
Pb1 sphere 1	O12	2.518(3)				
	O11	2.519(3)				
Pb1 sphere 2	O21	2.617(3)	O41	2.657(3)		
			O61	2.803(4)		
Pb1 sphere 3			O51	2.902(4)		
			O52	3.124(5)		
			O62	3.163(4)		
			O42	3.312(5)		
Pb2 sphere 1	O31	2.494(3)			O1	2.576(3)
Pb2 sphere 2	O32	2.656(3)	O81	2.626(4)		
			O71	2.721(3)		
			O101	2.800(3)		
			O72	2.803(3)		
Pb2 sphere 3			O82'	3.031(3)		
			O91	3.133(4)		
			O102	3.150(4)		
			O83	3.425(5)		

<sup>a</sup> Bond lengths included in coordination sphere 1: < 2.6 Å; coordination sphere 2: 2.6–2.9 Å; coordination sphere 3: 2.9–3.5 Å.

under a cold N<sub>2</sub> stream. X-ray diffraction data were obtained using a Bruker APEX II CCD detector/D8 diffractometer (for Pb-Val-Ile) or a Bruker SMART 1000 CCD detector/PLATFORM diffractometer (for all other compounds) using graphite-monochromated Mo K $\alpha$  radiation ( $\lambda = 0.71073$  Å). Programs for diffractometer operation, unit cell indexing, data collection, data reduction, and absorption correction were those supplied by Bruker. The data were corrected for absorption through Gaussian integration from indexing of the crystal faces. Structures were solved using the Patterson search/structure expansion facilities within the DIRDIF-99 program system.<sup>20</sup> Refinements were completed using the

program SHELXL-97.<sup>21</sup> Hydrogen atoms were assigned positions based on the geometries of their attached carbon, nitrogen, or oxygen atoms, and were given thermal parameters 20% (for C–H or N–H) or 50% (for O–H) greater than those of their parent atoms. For both structures an idealized geometry was imposed upon the water molecules by fixing the O–H bond distances at 1.00 Å and the intramolecular H···H distances at 1.63 Å during refinement. These water hydrogen atoms were oriented toward nearby nitrate group oxygen atoms by constraining the four atoms of the O–H···O–N hydrogen-bonded units to be coplanar (i.e., by setting these atoms to define a tetrahedron with a volume of no more than 0.001 Å<sup>3</sup>). See Table 1 for a

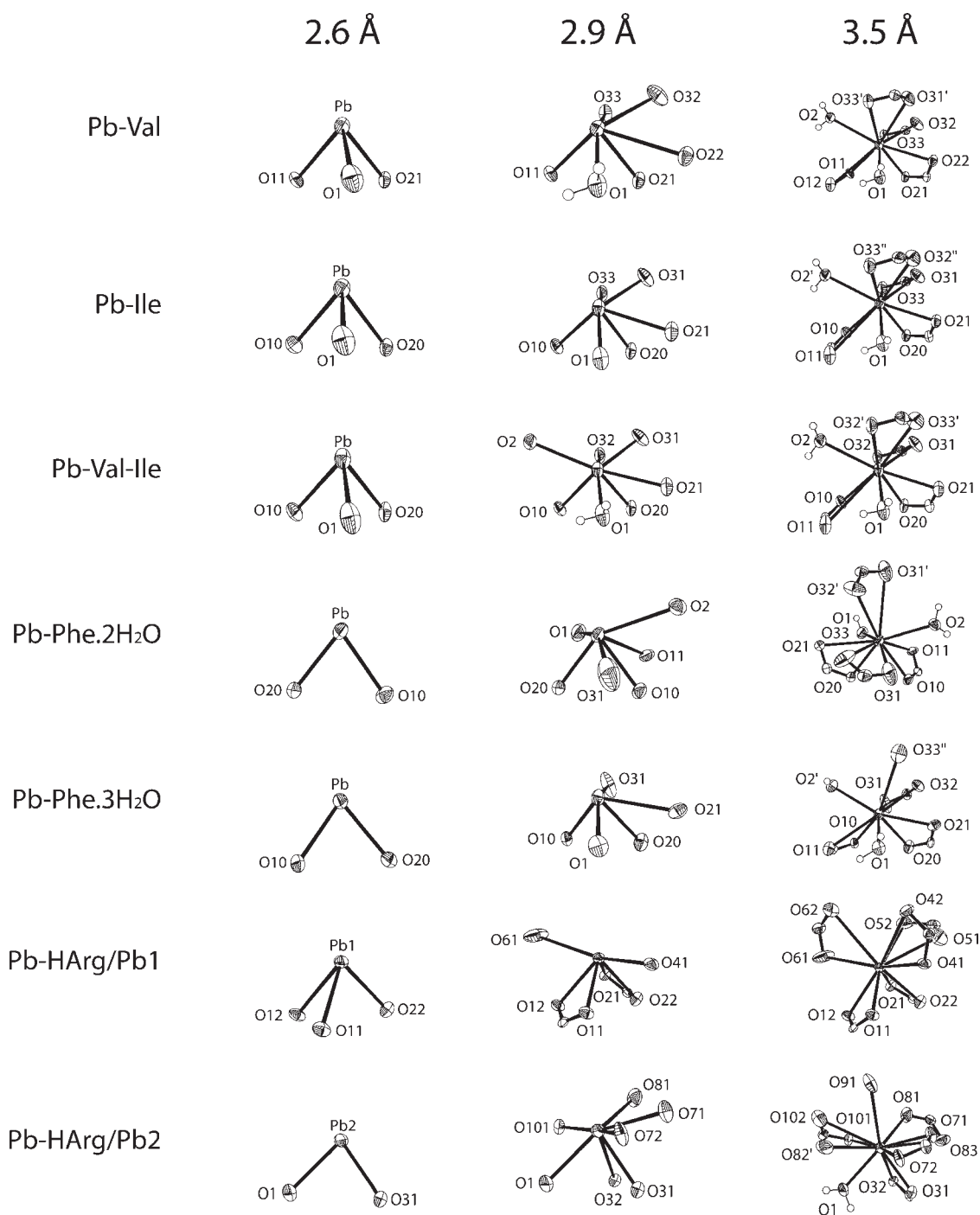


**Figure 5.** Comparison of the environments of the lead center in the solid state structures of lead-amino acid complexes, within sphere 1 (<2.6 Å), sphere 2 (2.6–2.9 Å), and sphere 3 (2.9–3.5 Å).

summary of crystal parameters for each complex. Views of the structures were prepared using Ortep 3 v2 for Windows<sup>22</sup> and Adobe Illustrator CS2.<sup>23</sup>

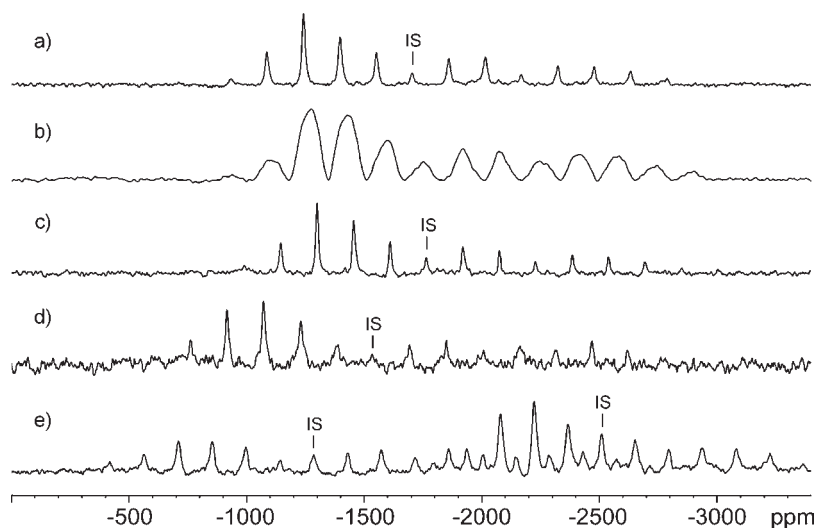
**Chemical Shift/pD Assessment for Solutions of Lead-Valine, L-Valine, and Lead Nitrate.** Solutions of L-valine, lead nitrate, or equimolar lead nitrate and L-valine mixtures in deuterium oxide at room temperature were prepared at a volume of 5.00 mL at 0.125 M with DSS added to a concentration of  $1.0 \times 10^{-2}$  M. Six values of pD (between 1 and 6) were accessed for each solution by addition of DNO<sub>3</sub> and/or NaOD. <sup>1</sup>H, <sup>13</sup>C, and <sup>207</sup>Pb NMR spectra were obtained at each pD value. Control solutions were prepared without DSS.

**Lead-207 Chemical Shift/Amino Acid to Lead Ratio Assessment for Lead-Valine.** Aqueous solutions of lead nitrate with L-valine (10.0 mL, 0.125 M Pb) with lead to valine ratios of 1:0, 1:0.5, 1:1, 1:1.5, 1:2, 1:3, 1:4, 1:5, and 1:6 ratio were prepared at room temperature. The pH of each solution was adjusted to 4.35 using HNO<sub>3</sub> or NaOH.

**Chemical Shift/Ionic Strength Assessment for Lead-Valine, L-Valine, and Lead Nitrate Solutions.** Solutions of L-valine, of lead nitrate, and of an equimolar mixture of lead nitrate with L-valine in deuterium oxide were prepared (4.00 mL, 0.125 M Pb or Val) at room temperature with DSS added to a concentration of  $1.0 \times 10^{-2}$  M.

**Table 3.** Solid State and Solution  $^{207}\text{Pb}$  Chemical Shifts of Lead Nitrate, Crystalline Samples of Lead-Amino Acid Complexes, Reaction Mixtures, or Dissolved Crystals at the Given pD Values and at 0.125 M Concentration of Lead

reaction mixture or Dissolved Crystals	solid state $^{207}\text{Pb}$ MAS NMR isotropic shift (ppm)	solution pD	solution $^{207}\text{Pb}$ NMR chemical shift (ppm)	solution lead:amino acid ratio
$\text{Pb}(\text{NO}_3)_2$	$-3490$ (T dependent) <sup>12</sup>	1 to 5	ca. $-2925$	1:0
$\text{Pb}(\text{NO}_3)_2 + \text{L-valine}$		4.63	$-2703$	1:1
$[\text{Pb}(\text{OH}_2)_2(\text{Val})_2(\text{NO}_3)][\text{NO}_3]$	$-1707 \pm 5$	4.9	$-2525$	1:2
$\text{Pb}(\text{NO}_3)_2 + \text{L-isoleucine}$		4.48	$-2693$	1:1
$[\text{Pb}(\text{OH}_2)_2(\text{Ile})_2(\text{NO}_3)][\text{NO}_3]$	$-1766 \pm 4$	5.0	$-2474$	1:2
$\text{Pb}(\text{NO}_3)_2 + \text{L-valine} + \text{L-isoleucine}$		4.50	$-2485$	1:2
$[\text{Pb}(\text{OH}_2)_2(\text{Val})(\text{Ile})(\text{NO}_3)][\text{NO}_3]$	(see Supporting Information)	4.9	$-2471$	1:2
$\text{Pb}(\text{NO}_3)_2 + \text{L-phenylalanine}$		4.36	$-2708$	1:1
$[\text{Pb}(\text{OH}_2)_2(\text{Phe})_2(\text{NO}_3)][\text{NO}_3]$	$-1541 \pm 5$	4.7	$-2536$	1:2
$\text{Pb}(\text{NO}_3)_2 + \text{L-arginine} + \text{DNO}_3$		2.78	$-2819$	1:1
$\text{Pb}_2(\text{HArg})_3(\text{H}_2\text{O})(\text{NO}_3)_7 \cdot 3\text{H}_2\text{O}$	Pb1: $-1285 \pm 5$ Pb2: $-2511 \pm 5$	4.7	$-2675$	1:1.5

**Figure 6.** Lead- $^{207}$  ssNMR spectra of ground crystals of (a)  $[\text{Pb}(\text{OH}_2)_2(\text{Val})_2(\text{NO}_3)][\text{NO}_3]$ , (b)  $[\text{Pb}(\text{OH}_2)_2(\text{Val})(\text{Ile})(\text{NO}_3)][\text{NO}_3]$ , (c)  $[\text{Pb}(\text{OH}_2)_2(\text{Ile})_2(\text{NO}_3)][\text{NO}_3]$ , (d)  $[\text{Pb}(\text{OH}_2)_2(\text{Phe})_2(\text{NO}_3)][\text{NO}_3]$ , (e)  $\text{Pb}_2(\text{HArg})_3(\text{H}_2\text{O})(\text{NO}_3)_7 \cdot 3\text{H}_2\text{O}$ . The isotropic shifts are marked with IS.

Sodium nitrate was added to four of the solutions to give five different ionic strengths between 0.38 and 0.88. The pD of each solution was adjusted with  $\text{DNO}_3$  and NaOD.

## RESULTS AND DISCUSSION

As a contribution toward the fundamental understanding of heavy metal-amino acid interactions, we have isolated and comprehensively characterized complexes of lead with L-valine, L-isoleucine,<sup>4</sup> L-phenylalanine, or L-arginine, as well as a complex involving both L-valine and L-isoleucine. Heated (95–100 °C) mixtures of each amino acid with lead nitrate in water result in colorless solutions that give crystals by slow cooling and evaporation. In the case of L-arginine, it was necessary to acidify the solution with nitric acid until the solution became clear (pH ca. 3), prior to heating. The compounds have been identified by X-ray crystallography as  $[\text{Pb}(\text{OH}_2)_2(\text{Val})_2(\text{NO}_3)][\text{NO}_3]$ ,  $[\text{Pb}(\text{OH}_2)_2(\text{Phe})_2(\text{NO}_3)][\text{NO}_3]$ ,  $\text{Pb}_2(\text{HArg})_3(\text{H}_2\text{O})(\text{NO}_3)_7 \cdot 3\text{H}_2\text{O}$ , and  $[\text{Pb}(\text{OH}_2)_2(\text{Val})(\text{Ile})(\text{NO}_3)][\text{NO}_3]$ , respectively. A sample of  $[\text{Pb}(\text{OH}_2)_2(\text{Phe})_2(\text{NO}_3)][\text{NO}_3] \cdot \text{H}_2\text{O}$  (see Supporting Information) has also been crystallographically

characterized; however, it was not possible to reproduce the sample. The structure of  $[\text{Pb}(\text{OH}_2)_2(\text{Ile})_2(\text{NO}_3)][\text{NO}_3]$  was also determined (see Supporting Information) and has been previously reported.<sup>4</sup> Solid samples have been characterized using IR, Raman, and CP-MAS NMR spectroscopy. Aqueous solutions of dissolved crystals and reaction mixtures have been characterized using NMR spectroscopy and ESI-MS.

The solid state structures of Pb-Val, Pb-Val-Ile, Pb-Phe  $\cdot$  2  $\text{H}_2\text{O}$ , and Pb-HArg all contain a lead center complexed by one or more amino acid ligands, water and nitrate ions, consistent with the structure of Pb-Ile.<sup>4</sup> The asymmetric units of Pb-Val, Pb-Val-Ile, Pb-Phe  $\cdot$  2  $\text{H}_2\text{O}$ , and Pb-HArg are illustrated in Figures 1 to 4. The oxygen enclosed lead environments in each of the compounds and Pb-Ile are illustrated and compared in Figure 5, within three coordination spheres for Pb, listed in Table 2 for Pb–O distances less than 2.6 Å (sphere 1), Pb–O distances between 2.6 Å and 2.9 Å (sphere 2), and Pb–O distances between 2.9 Å and 3.5 Å (sphere 3). While the geometry of the lead center in all compounds is hemidirected<sup>24</sup> (ligands on one side of the lead center) within sphere 2, each lead center is

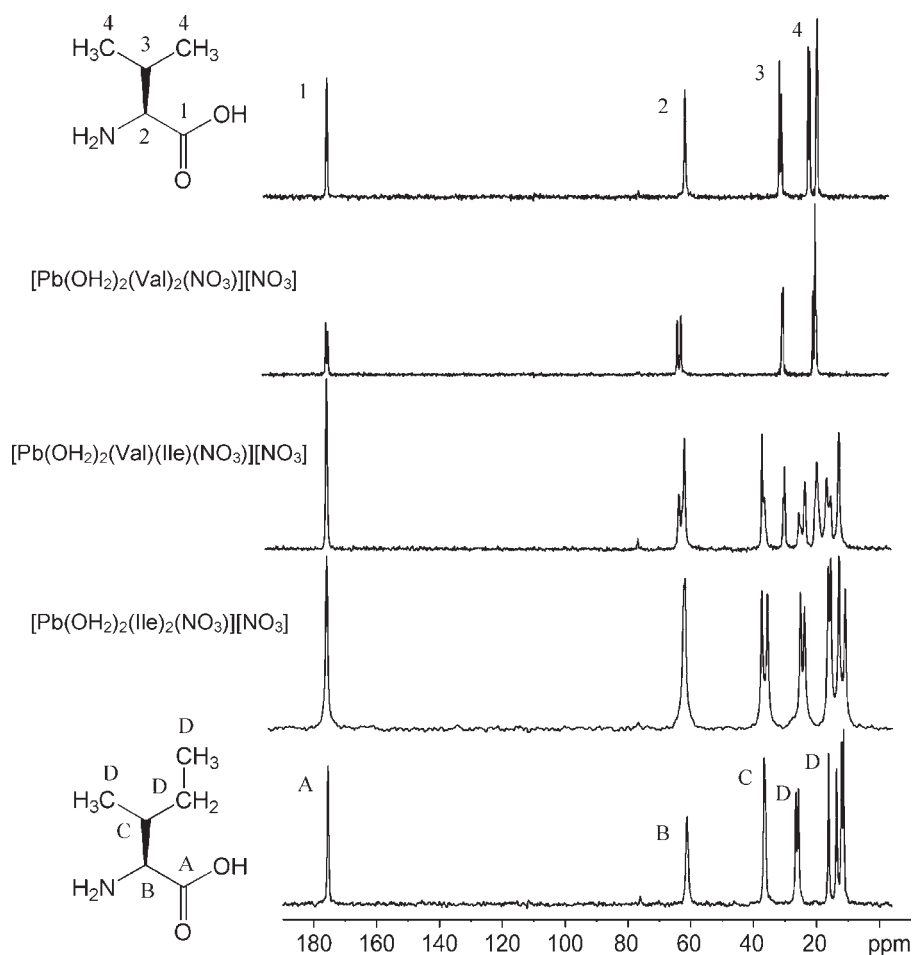


**Figure 7.** Carbon-13 CP-MAS NMR spectra of L-valine,  $[\text{Pb}(\text{OH}_2)_2(\text{Val})_2(\text{NO}_3)][\text{NO}_3]$ ,  $[\text{Pb}(\text{OH}_2)_2(\text{Val})(\text{Ile})(\text{NO}_3)][\text{NO}_3]$ ,  $[\text{Pb}(\text{OH}_2)_2(\text{Ile})_2(\text{NO}_3)][\text{NO}_3]$ , and L-isoleucine. Labels 1, 2, 3 and A, B, C, D refer to the isotropic shifts for the pure L-valine and L-isoleucine, respectively.

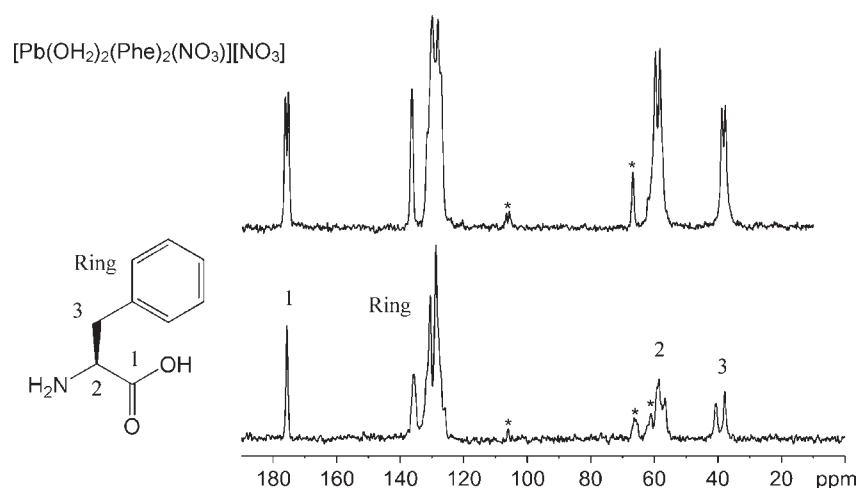


**Figure 8.** Carbon-13 CP-MAS NMR spectra of  $[\text{Pb}(\text{OH}_2)_2(\text{Phe})_2(\text{NO}_3)][\text{NO}_3]$ , and L-phenylalanine. The isotropic shifts for the pure amino acid are labeled, and the asterisk refers to spinning sidebands (\*).

holodirected within the sum of the van der Waals radii for  $\text{Pb}\cdots\text{O}$  (sphere 3, 2.9–3.5 Å). In this context, the assignment of the environment of lead in these compounds as hemi- or holo-directed is arbitrary, and the extent of the data (number of

examples) is insufficient to interpret the influence of the coordination sphere on the chemistry at the lead center.

In the structure of Pb-Val (Figure 1), the lead center interacts with two valine carboxylate units (O21 and O11) and a water



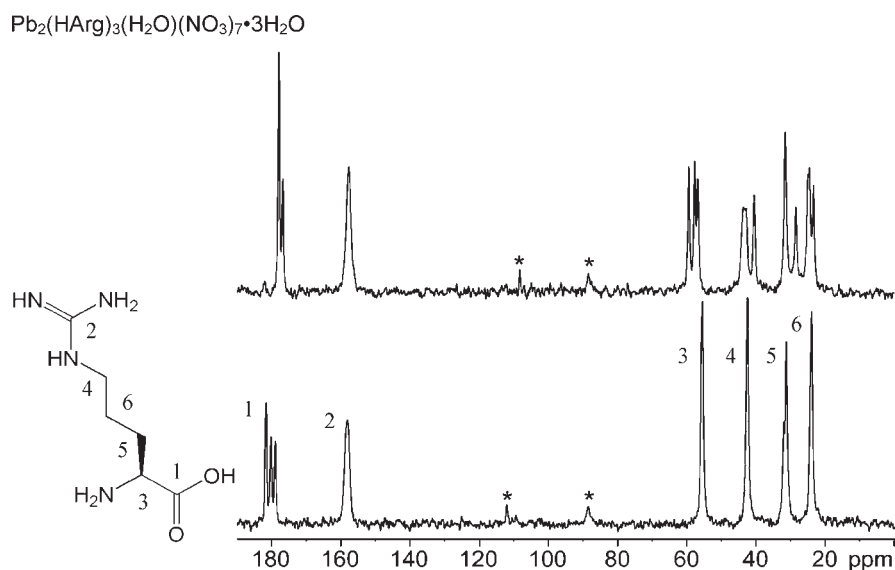


**Figure 9.** Carbon-13 CP-MAS NMR spectra of  $\text{Pb}_2(\text{OH}_2)(\text{HArg})_3(\text{NO}_3)_7 \cdot 3\text{H}_2\text{O}$  and L-arginine. The isotropic shifts for the pure amino acid are labeled, and the asterisk refers to spinning sidebands (\*).

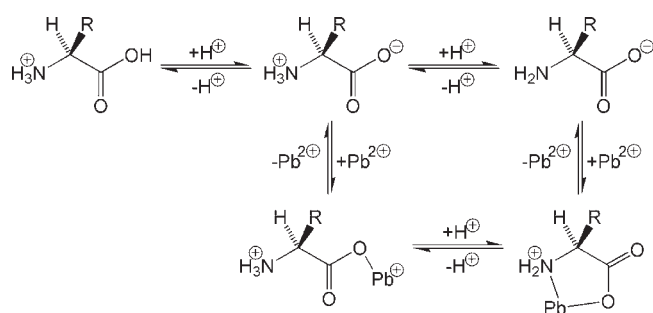


**Figure 10.** Dissociation equilibria for an amino acid in the presence of lead.

molecule (O1), with acute angles at lead (O1–Pb–O11  $88.24(8)^\circ$ , O1–Pb–O21  $79.81(8)^\circ$ , and O11–Pb–O21  $76.26(8)^\circ$ ). Coordination sphere 2 ( $\leq 2.9 \text{ \AA}$ ) introduces a chelate interaction of a valine carboxylate group (O22), a chelate interaction from a nitrate counterion (O33 and O32) and interaction with a second water molecule (O2). The amine of the neutral zwitterionic L-valine ligands is protonated and does not interact with the lead center. Within the crystal lattice, the isopropyl substituents of the valine ligands are aligned into a hydrophobic plane (Supporting Information).

The structure of Pb-Ile contains a lead center interacting with a carboxylate group from each of two isoleucine ligands (O20 and O10) and one water molecule (O1), giving acute bond angles of  $76.30(8)^\circ$  (O10–Pb–O20),  $79.55(9)^\circ$  (O1–Pb–O20), and  $84.79(9)^\circ$  (O1–Pb–O10). Sphere 2 involves a second oxygen center from one carboxylate group (O21), and a chelated nitrate anion (O33 and O31). A chelate interaction to the same nitrate anion of the next asymmetric unit (O32'' and O33''), an interaction with a second oxygen center from the carboxylate group (O11) and a second water molecule (O2') impose a formal ten coordinate environment for lead. The butyl side chains of the isoleucine molecules are aligned into a hydrophobic plane through the crystal lattice (Supporting Information).

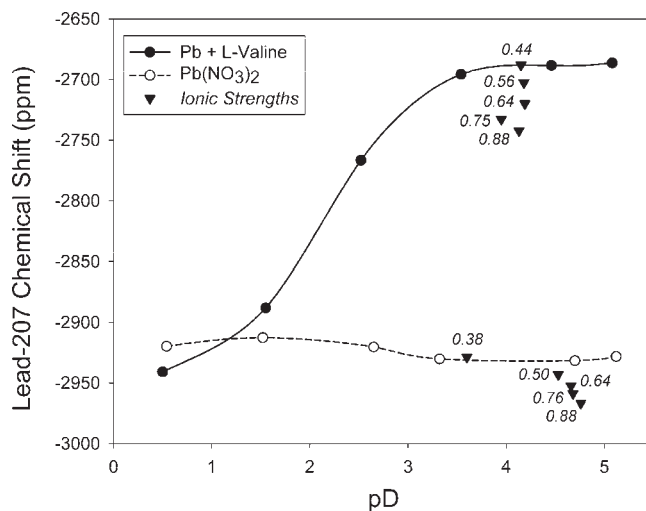


**Figure 11.** Change in lead-207 chemical shift nitrate with increasing pD values (and increasing solution ionic strength) of a lead nitrate with L-valine solution and a lead solution.

The structure of Pb-Val-Ile (Figure 2) contains a lead center interacting a carboxylate group on each of the valine (O20) and isoleucine molecules (O10) and from a water molecule (O1). The bond angles are acute within sphere 1 [ $75.73(11)^\circ$  (O10–Pb–O20),  $80.15(12)^\circ$  (O1–Pb–O20) and  $85.11(11)^\circ$  (O1–Pb–O10)]. Sphere 2 involves a second oxygen from one carboxylate group (O21), an additional water molecule (O2), and two oxygen atoms (O31 and O32) from a nitrate counterion. A nitrate counterion from the adjacent asymmetric unit (O33' and O32') forms a two-dimensional chain of alternating lead atoms and nitrate counterions, and interactions with the remaining carboxylate oxygen atom from the isoleucine molecule (O11) occur within sphere 3. As for Pb-Ile and Pb-Val, the R-groups of the amino acids are aligned into a hydrophobic plane through the crystal lattice (Supporting Information).

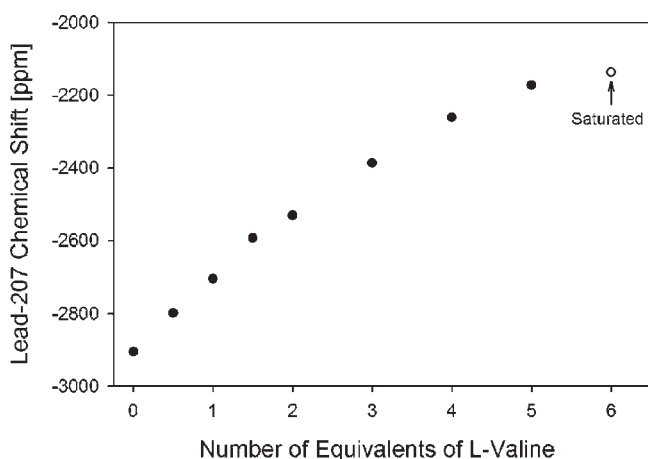


**Figure 12.** Change in lead-207 chemical shift with decreasing lead to valine ratios; to the valine saturation point which is at a ratio between 1:5 and 1:6.

In  $\text{Pb} \cdot \text{Phe} \cdot 2\text{H}_2\text{O}$ , one lead center is bound by two zwitterionic phenylalanine molecules, two nitrate counteranions and two water molecules (Figure 3). The closest interactions ( $\leq 2.6$  Å) involve the carboxylate group of each phenylalanine molecule (O20 and O10) with a O10–Pb–O20 bond angle of  $73.05(11)^\circ$ . The second coordination sphere ( $\leq 2.9$  Å) involves two water molecules (O1 and O2), one carboxylate group (O11), and a nitrate anion (O31). The other carboxylate oxygen (O21), a second oxygen from the nitrate counterion (O33), and a nitrate ion from an adjacent asymmetric unit (O32' and O31') to engage lead in the third coordination sphere. The phenyl rings are situated perpendicular to each other along the crystal lattice, as shown in the side view in Figure 3. Crystals of  $[\text{Pb}(\text{OH}_2)_2(\text{Phe})_2(\text{NO}_3)][\text{NO}_3] \cdot \text{H}_2\text{O}$  were isolated on only one occasion (Supporting Information).

The asymmetric unit of  $\text{Pb}_2(\text{HArg})_3(\text{H}_2\text{O})(\text{NO}_3)_7 \cdot 3\text{H}_2\text{O}$  (Figure 4) contains two lead centers, three protonated arginine molecules (protonated amine and guanidinium groups, and a deprotonated carboxylate group), seven nitrate counteranions, and four water molecules. The Pb1 center interacts with two arginine molecules through the carboxylate groups, while the Pb2 center interacts with the carboxylate group of only one arginine molecule. This structure represents the first report of the interaction of lead with a cationic amino acid ligand. The local environment at Pb1 (within 2.6 Å) involves two carboxylate groups (O11, O12, and O22), with acute bond angles (O11–Pb1–O12  $52.10(9)^\circ$ , O11–Pb1–O22  $79.04(10)^\circ$ , and O12–Pb1–O22  $80.55(10)^\circ$ ). Sphere 2 involves the remaining carboxylate group oxygen atom (O21) and two nitrate ions (O41 and O61). Four interactions from three nitrate ions (O51, O52, O62, and O42) are within sphere 3.

The local environment of Pb2 ( $\leq 2.6$  Å) involves only one carboxylate group (O31) and one water molecule (O1), with an acute bond angle of  $76.39(10)^\circ$  (O1–Pb2–O31). Sphere 2 contains the second carboxylate group oxygen (O32) and four interactions with nitrate ions (O81, O71, O101, and O72), and sphere 3 includes interactions from four nitrate counterions (O82', O91, O102, and O83). The cationic, planar guanidinium units interact with nitrate ions and form a layered structure (Supporting Information).

Solid state  $^{13}\text{C}$  and  $^{207}\text{Pb}$  CP-MAS NMR spectra were obtained for all crystalline samples. The spectroscopic data are

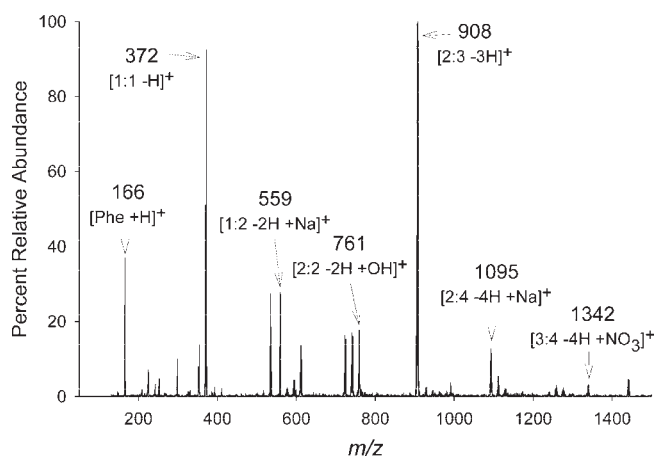


**Figure 13.** ESI mass spectrum of  $[\text{Pb}(\text{OH}_2)_2(\text{Phe})_2(\text{NO}_3)][\text{NO}_3]$  crystals dissolved in water with water as the flow solvent (maximum ion intensity  $1.50 \times 10^5$ ). Peaks are labeled with  $m/z$  value and the associated complex cation; ratios are in the form of metal to amino acid.

consistent with X-ray crystallography data and confirm that the individual crystals are representative of the bulk crystalline material. In general, samples exhibit a  $^{207}\text{Pb}$  isotropic shift (Table 3) assigned to the complex as well as a signal corresponding to lead nitrate ( $-3490$  ppm), which is an impurity in the samples, but provides a useful internal reference. Figure 6 compares the solid state  $^{207}\text{Pb}$  spectra for all compounds. The comparison between these spectra highlights the sensitivity of the  $^{207}\text{Pb}$  chemical shifts to the lead environments within the crystal structures. For example, the  $^{207}\text{Pb}$  isotropic chemical shifts of the compounds containing formally neutral amino acids, Pb-Val, Pb-Ile, and Pb-Phe are within 250 ppm of each other, consistent with the similarity of the lead environments.

The  $^{13}\text{C}$  CP/MAS NMR spectra of the lead-amino acid complexes differ only slightly from those of the pure amino acid (Figures 7, 8, 9). For each complex, the number of signals is consistent with the symmetry of the solid state structure determined using X-ray crystallography. For example, the asymmetric unit of Pb-Val contains pairs of nonsymmetric carbon atoms in five chemically distinct environments, potentially giving 10 signals in the  $^{13}\text{C}$  CP/MAS NMR spectrum. The  $^{13}\text{C}$  CP/MAS NMR spectrum for these crystals contains seven distinct signals (Figure 8), of which three result from the overlap of six nonsymmetric carbon signals. As expected,  $^{13}\text{C}$  CP/MAS NMR spectra for Pb-Val-Ile presents a combination of features observed for Pb-Val and Pb-Ile (Figure 8). The  $^{13}\text{C}$  CP/MAS spectrum of the mixed amino acid compound Pb-Val-Ile shows sharp lines indicating a nicely crystalline material.

In acidic solution, protons compete with lead ions for the donor atoms of the amino acid (Figure 10). To confirm the existence of the lead-amino acid interaction in solution,  $^1\text{H}$ ,  $^{13}\text{C}$ , and  $^{207}\text{Pb}$  NMR spectra were obtained for solutions of crystals dissolved in deuterium oxide and for reaction mixtures prepared in deuterium oxide (with measured pD values). These spectra were compared to those of solutions of the free amino acid or lead nitrate at the same (or similar) pD values, and do not show significant chemical shift differences.

The  $^{207}\text{Pb}$  NMR chemical shift of the lead nitrate solution is essentially independent of pD (or pH), while solutions of lead nitrate with L-valine exhibit a downfield shift as the pD of the solution is increased, as shown in Figure 11. The  $^{207}\text{Pb}$  signal was

**Table 4. Positive Ion ESI-MS Data with Assignments for  $m/z$  Peaks for Solutions of Crystals and Reaction Mixtures**

lead-amino acid	$m/z$	complex cation assignment [Pb:amino acid]
Pb-Val	324	[1:1 -H] <sup>+</sup>
	463	[1:2 -2H +Na] <sup>+</sup>
	665	[2:2 -2H +OH] <sup>+</sup>
	764	[2:3 -3H] <sup>+</sup>
	903	[2:4 -4H +Na] <sup>+</sup>
	1150	[3:4 -4H +NO <sub>3</sub> ] <sup>+</sup>
Pb-Ile	338	[1:1 -H] <sup>+</sup>
	491	[1:2 -2H +Na] <sup>+</sup>
	693	[2:2 -2H +OH] <sup>+</sup>
	804	[2:3 -3H] <sup>+</sup>
	959	[2:4 -4H +Na] <sup>+</sup>
	1206	[3:4 -4H +NO <sub>3</sub> ] <sup>+</sup>
Pb-Val-Ile	324	[1:1:0 -H] <sup>+</sup>
	338	[1:0:1 -H] <sup>+</sup>
	441	[1:2:0 -H] <sup>+</sup>
	455	[1:1:1 -H] <sup>+</sup>
	469	[1:0:2 -H] <sup>+</sup>
	477	[1:1:1 -2H +Na] <sup>+</sup>
	491	[1:0:2 -2H +Na] <sup>+</sup>
	679	[2:1:1 -2H +OH] <sup>+</sup>
	693	[2:0:2 -2H +OH] <sup>+</sup>
	764	[2:3:0 -3H] <sup>+</sup>
	778	[2:2:1 -3H] <sup>+</sup>
	792	[2:1:2 -3H] <sup>+</sup>
	806	[2:0:3 -3H] <sup>+</sup>
	931	[2:2:2 -4H +Na] <sup>+</sup>
	945	[2:1:3 -4H +Na] <sup>+</sup>
	959	[2:0:4 -4H +Na] <sup>+</sup>
1178	[3:2:2 -4H +NO <sub>3</sub> ] <sup>+</sup>	
1192	[3:1:3 -4H +NO <sub>3</sub> ] <sup>+</sup>	
1206	[3:0:4 -4H +NO <sub>3</sub> ] <sup>+</sup>	
Pb-Phe	372	[1:1 -H] <sup>+</sup>
	559	[1:2 -2H +Na] <sup>+</sup>
	761	[2:2 -2H +OH] <sup>+</sup>
	908	[2:3 -3H] <sup>+</sup>
	1095	[2:4 -4H +Na] <sup>+</sup>
	1342	[3:4 -4H +NO <sub>3</sub> ] <sup>+</sup>
Pb-HArg	381	[1:1 -H] <sup>+</sup>
	555	[1:2 -H] <sup>+</sup>
	824	[2:2 -2H +NO <sub>3</sub> ] <sup>+</sup>
	935	[2:3 -3H] <sup>+</sup>

also affected by the concentration of amino acid in solution. Sequential addition of *L*-valine to aqueous solutions of lead nitrate (at 0.125 M Pb and pH 4.26 to 4.44, Figure 12) resulted in about 800 ppm downfield shift up to solution saturation. A distinct <sup>207</sup>Pb downfield shift was observed for the reaction mixtures of Pb(NO<sub>3</sub>)<sub>2</sub> with each of the amino acids (0.125 M amino acid), and for the dissolved crystals (at 0.125 M Pb) (Table 3), which we attribute to interaction between the amino acid and lead.

Changes in ionic strength of the solution at pD about 4 had no effect on the internally calibrated <sup>13</sup>C shift ( $\Delta\delta_{\text{DSS}} = 174.8$  ppm to 174.9 ppm). The externally calibrated lead-207 chemical shifts are

upfield over a range of 54 ppm with increasing ionic strength over a range of 0.38 to 0.88;<sup>25</sup> however, changes in pD have a larger effect on the <sup>207</sup>Pb chemical shifts (−2686 ppm at pD 5.08 compared to −2941 ppm at pD 0.50), Figure 11.

ESI-MS data was obtained for reaction mixtures of lead nitrate with *L*-valine, *L*-isoleucine, or *L*-phenylalanine, for an acidified reaction mixture of lead nitrate with *L*-arginine and for aqueous and methanolic solutions of crystals of Pb-Val, Pb-Ile, Pb-Val-Ile, Pb-Phe, and Pb-HArg. A representative ESI mass spectrum for a solution of crystals of Pb-Phe with aqueous flow solvent, is presented in Figure 13. In this spectrum, the protonated phenylalanine signal is indicated at  $m/z$  166, and the peaks relating to complexes containing both lead and amino acid are labeled.

Table 4 provides a summary of the solution mass analyses. Mass to charge peaks are assigned only to complex cations containing both lead and amino acid. The observed peaks are independent of flow solvent (distilled water and 50% methanol/water (v/v)). Peak assignments have been made by comparing experimental and calculated isotope peak patterns, as well as observed tandem mass spectra for selected peaks. Assignments are listed as ratios of lead to amino acid. The single positive charge on the cation is balanced by loss of  $x$  number of protons ( $-x\text{H}$ ), or by association with a nitrate, sodium or hydroxide ion.

The 1:2 lead:amino acid ratio present in solid state structures and the 1:1:1 lead:valine:isoleucine ratio in the solid state structure of Pb-Val-Ile are also apparent in cations observed in the gas phase. The 1:1 lead to amino acid ratio speculated in the solution state is also evident in the gas phase. Additional gas phase complex cations are present at larger mass to charge ratios, which imply the presence of clusters of the smaller complex cations. Gas phase analyses of the lead-valine-isoleucine dissolved crystals and reaction mixture show the presence of complex cations with a combination of valine and/or isoleucine ligands.

## CONCLUSIONS

Four new lead-amino acid complexes have been isolated from acidic aqueous lead-amino acid solutions and have been comprehensively characterized in the solid state, the solution state, and the gas phase. The complexes of the neutral amino acids Val, Ile, and Phe contain one lead center coordinated by two amino acids, while the lead and cationic arginine (HArg) complex is a cluster containing two lead centers and three arginine molecules. Lead-207 NMR isotropic shifts in the solid and solution states correlate with the number of amino acids and water molecules interacting with the lead center, and a 1:1 lead to amino acid interaction is speculated in solution. The solution state <sup>1</sup>H, <sup>13</sup>C, and <sup>207</sup>Pb chemical shifts are strongly affected by the pD of the solution. The lead to amino acid ratios observed in the solid state are observed in the gas phase. The comprehensive characterization data for these complexes provide a foundation to develop an understanding of chemical interactions between heavy metals and amino acids.

## ASSOCIATED CONTENT

**S Supporting Information.** Crystallographic data in CIF format. Further details are given in Figures S.1–S.20. This material is available free of charge via the Internet at <http://pubs.acs.org>.

## AUTHOR INFORMATION

### Corresponding Author

\*Phone: (902) 494-3707. Fax: (902) 494-1310. E-mail: neil.burford@dal.ca.

## ACKNOWLEDGMENT

The authors thank the NMR-3 and the Dalhousie Mass Spectrometry Laboratories for use of instrumentation, Wesley LeBlanc and Melanie Eelman for preliminary experimental work and the Natural Sciences and Engineering Research Council of Canada, the Canada Research Chairs program, the Canada Foundation for Innovation, and the Nova Scotia Research and Innovation Trust Fund for financial support.

## REFERENCES

- (1) Phillip, A. T.; Gerson, B. *Clin. Lab. Med.* **1994**, *14*, 423–444.
- (2) Gasque, L.; Bernes, S.; Ferrari, R.; de Barbarin, C. R.; de Jesus Gutierrez, M.; Mendoza-Diaz, G. *Polyhedron* **2000**, *19*, 649–653.
- (3) Marandi, F.; Shahbakhsh, N. *Z. Anorg. Allg. Chem.* **2007**, *633*, 1137–1139.
- (4) Gasque, L.; Verhoeven, M. A.; Bernes, S.; Barrios, F.; Haasnot, J. G.; Reedijk, J. *Eur. J. Inorg. Chem.* **2008**, 4395–4403.
- (5) Marandi, F.; Shahbakhsh, N. *J. Coord. Chem.* **2007**, *60*, 2589–2595.
- (6) Freeman, H. C.; Stevens, G. N.; Taylor, I. F. *J. Chem. Soc., Chem. Commun.* **1974**, 366–367.
- (7) Ye., Q.; Li, Y.-H.; Wu, Q.; Song, Y.-M.; Wang, J.-X.; Zhao, H.; Xiong, R.-G.; Xue, Z. *Chem.—Eur. J.* **2005**, *11*, 988–994.
- (8) Nakashima, T. T.; Rabenstein, D. L. *J. Magn. Reson.* **1983**, *51*, 223–232.
- (9) Shindo, H.; Brown, T. L. *J. Am. Chem. Soc.* **1965**, *87*, 1904–1909.
- (10) Kane-Maguire, L. A. P.; Riley, P. J. *J. Coord. Chem.* **1993**, *28*, 105–120.
- (11) Burford, N.; Eelman, M. D.; LeBlanc, W. G.; Cameron, T. S.; Robertson, K. N. *Chem. Commun.* **2004**, 332–333.
- (12) Beckmann, P. A.; Dybowski, C. *J. Magn. Reson.* **2000**, *146*, 379–380.
- (13) *xedplot Program*; Bruker: Madison, WI.
- (14) Grimmer, A.-R.; Kretschmer, A.; Cajipe, V. B. *Magn. Reson. Chem.* **1997**, *35*, 86–90.
- (15) Harris, R. K.; Becker, E. D.; Cabared de Menezes, S. M.; Goodfellow, R.; Granger, P. *Pure Appl. Chem.* **2001**, *73*, 1795–1818.
- (16) Yan, J. *Isotope Pattern Calculator*, v4.0; Ohio State University: Columbus, OH, 2001; Available online at <http://www.geocities.com/junhuayan/pattern.htm>.
- (17) *Qual Browser*, v 1.2; Finnigan Corporation: Waltham, MA, 1998–2000.
- (18) *Excel 2002*; Microsoft Corporation: Redmond, WA, 1985–2001.
- (19) *Sigma Plot*, v10.0; Systat Software, Inc.: Chicago, IL, 2006.
- (20) Beurskens, P. T.; Beurskens, G.; de Gelder, R.; Garcia-Granda, S.; Israel, R.; Gould, R. O.; Smits, J. M. M. *The DIRDIF-99 program system*; Crystallography Laboratory, University of Nijmegen: Nijmegen, The Netherlands, 1999.
- (21) Sheldrick, G. M. *SHELXL-97*; University of Göttingen: Göttingen, Germany, 1997.
- (22) Farrugia, L. J. *Appl. Crystallogr.* **1997**, *30*.
- (23) *Adobe Illustrator CS2*, v12.0.1; Adobe Systems Inc.: San Jose, CA, 1987–2005.
- (24) Shimoni-Livny, L.; Glusker, J. P.; Bock, C. W. *Inorg. Chem.* **1998**, *37*, 1853–1867.
- (25) Stellwagen, E.; Prantner, J. D.; Stellwagen, N. C. *Anal. Biochem.* **2008**, *373*, 407–409.